

Characterization of the Effective Torque Profile Associated With Driving Intrinsic Rotation on DIII-D

W.M. Solomon 1), K.H. Burrell 2), J.S. deGrassie 2), J.A. Boedo 3), P.H. Diamond 3), A.M. Garofalo 2), T.S. Hahm 1), R.A. Moyer 3), S.H. Muller 3), C.C. Petty 2), H. Reimerdes 4), G.R. Tynan 3), and R.E. Waltz 2)

1) Princeton Plasma Physics Laboratory, Princeton, New Jersey 08543-0451, USA

2) General Atomics, San Diego, California 92186-5608, USA

3) University of California at San Diego, La Jolla, California 92093-0424, USA

4) Columbia University, New York, New York 10027, USA

e-mail contact of main author: solomon@fusion.gat.com

Abstract. Recent experiments on DIII-D have focused on elucidating the drive mechanisms for intrinsic rotation in tokamak fusion plasmas. For a wide range of DIII-D H-mode plasmas, the effective torque at the edge ($\rho > 0.8$) associated with the intrinsic rotation shows a dependence on the edge pressure gradient, which is qualitatively consistent with models describing $E \times B$ shear as a means of creating “residual stress” and in turn driving intrinsic rotation. This is not the full picture, however, as recent probe measurements indicate that additional mechanisms may be necessary to completely understand edge intrinsic rotation generation. The intrinsic torque in the core ($\rho < 0.5$) of H-mode plasmas appears to be much more complex than the edge. Even though the core intrinsic torque tends to be much smaller than observed at the edge, some examples have been found where it is large enough to modify the rotation profile. For instance, in certain plasmas with electron cyclotron heating, a significant counter intrinsic torque has been observed in the inner region of the plasma. Large intrinsic torques have also been observed in the core of quiescent H-mode (QH-mode) plasmas and hybrid scenario plasmas. Studies of the residual stress with the global gyrokinetic code GYRO, have uncovered a novel result; namely that nonlocal profile variations appear capable of generating large residual stresses and associated momentum flows.

1. Introduction

Toroidal rotation in fusion plasmas is now widely acknowledged as being capable of delivering benefits to performance through improvements in both stability [1] and confinement [2]. In most present day tokamaks, rapid rotation is usually provided as a by-product of neutral beam heating, but as fusion moves toward ITER and the burning plasma era, the external torque applied by neutral beam heating systems is expected to become comparatively smaller. Therefore, plasma scenarios of future burning experiment may require re-optimization for low rotation operation unless alternate means of driving rotation are exploited. One possibility that has received attention in recent years is that the plasma itself might be capable of self-generating toroidal rotation, manifested by the observation of so-called “intrinsic rotation” [3]. This paper focuses on describing the effective torque profile associated with driving such intrinsic rotation in DIII-D.

The toroidal velocity V_ϕ evolves according to the angular momentum balance equation, which in simplified form can be written as $mR \partial n V_\phi / \partial r = \Sigma \eta - \nabla \cdot \Pi_\phi$, where η represents the various momentum sources, and Π_ϕ is the toroidal angular momentum flux. This flux can result for example by classical, neoclassical and turbulence effects,

$$\Pi_\phi = -mnR \left(\chi_\phi \frac{\partial V_\phi}{\partial r} - V_{\text{pinch}} V_\phi \right) + \Pi_{RS} \quad (1)$$

where V_ϕ is the toroidal velocity, χ_ϕ is the momentum diffusivity, V_{pinch} represents a pinch of angular momentum, Π_{RS} is the so-called “residual stress”, and other variables are of standard usage. The residual stress can simply be considered the component of momentum flux that is not proportional to either V_ϕ or its radial derivative. Because of this property, it

has been recognized that the residual stress may serve as an effective drive for intrinsic rotation. Theoretical work has considered various mechanisms capable of generating residual stress, including $E \times B$ shear [4,5], geometrical up-down asymmetries [6], fluctuation amplitude gradients [7], charge separation from the polarization drift [8], and ion temperature gradient variation [9]. Additional processes may also lead to effective sources of angular momentum. For example, thermal ion orbit loss of counter-current going ions may leave a hole in velocity space, resulting in co-current rotation [10].

2. Intrinsic Rotation Drive Near the Boundary

Measurements at the edge of DIII-D H-mode plasmas find that the edge intrinsic torque, defined here as the volume integral of the intrinsic torque density, $T_{\text{intrinsic}}^{\text{edge}} = \int_{\rho=0.8}^1 \eta_{\text{intrinsic}} dV$, is proportional to the edge pressure gradient as shown in Fig. 1. The data was obtained by slowly sweeping the neutral beam torque in DIII-D H-mode plasmas to find conditions whereby the plasma rotation is effectively zeroed out across the profile. Under these conditions, the intrinsic torque is approximately the negative of the externally applied neutral beam torque, a technique used previously to demonstrate the existence of the intrinsic torque [11]. The experiment was conducted using β_N feedback control to maintain constant β_N while the torque was being swept (by varying the balance of co and counter neutral beam injection). The neutral beam torque is calculated within TRANSP [12] using the NUBEAM package [13,14], and includes classical fast ion transport, and accounts for losses associated with shine through and direct orbit loss. As was noted in Ref. [11], non-classical fast ion transport, which is, for example, associated with Alfvén eigenmode instabilities, can quantitatively alter the calculated neutral beam torque profile, and with it, the inferred intrinsic torque. Even in these cases, however, the qualitative interpretation of the intrinsic torque is not dramatically altered, although the details clearly can be. Nonetheless, to minimize these complications, the plasmas included in this dataset have low (undetectable) level of Alfvén eigenmode activity and the calculated neutron rates were within error bars of the measured neutron rates. Under these conditions, the neutral beam model used within TRANSP can be expected to reliably compute the imparted torque.

In the plasmas studied here, with nominally zero toroidal rotation, the radial electric field arises predominantly from the pressure gradient. Therefore, the observed dependence of the edge intrinsic torque on the pressure gradient is qualitatively consistent with the theoretical picture of $E \times B$ shear driving residual stress and intrinsic rotation. If the edge pressure gradient is indeed capable of producing residual stress and spinning up the plasma, then an immediate consequence of this is that the H-mode pedestal may provide a ubiquitous mechanism for providing intrinsic rotation in fusion plasmas.

An important question is what role, if any, does this edge intrinsic drive play in plasmas where external momentum is input from neutral beam injection (NBI). An obvious limitation with the original technique for determining the intrinsic torque is that it can only be applied to plasmas where the rotation can be effectively zeroed out. To overcome this, an alternate

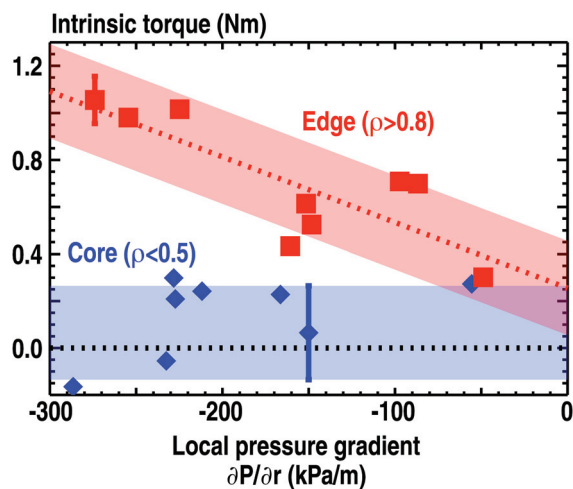


FIG. 1. The intrinsic torque at the edge of the plasma shows a strong correlation with the edge pressure gradient. No obvious correlation exists in the core, where the torque is typically negligible.

procedure for estimating the intrinsic torque in plasmas with finite rotation has been developed. The concept is to apply a step in the applied NBI torque step, preferably a small perturbation to minimize the changes to the background transport. For any assumed level of intrinsic torque, one can determine the momentum confinement time $\tau_\phi = L / (T_{\text{NBI}} + T_{\text{intrinsic}})$, where $L = \int nmRV_\phi dV$ is the total angular momentum, in the stationary part of the discharge. The momentum confinement time so determined should also properly describe the relaxation of the rotation immediately following the torque step. Hence, one can determine the level of intrinsic torque required to obtain a momentum confinement time that is consistent both during the steady and transient part of the discharge. To some extent, the intrinsic torque so-determined can be considered the “missing” torque required to make the steady state and transient momentum confinement times equal. Of course, it is not *a priori* clear that this simple model is able to capture the physics of the complete angular momentum balance equation and accurately reproduce the intrinsic torque profile. To validate the technique, it has been benchmarked in plasmas where the rotation profile was successfully brought to zero. The intrinsic torque profile obtained from this approach is found to be quantitatively comparable (as described in Ref. 15).

Using this approach, the role of intrinsic drive in plasmas with finite rotation has been investigated. At constant β_N , the rotation was varied by changing the balance of co and counter neutral beam injection. The results from this scan are presented in Fig. 2, with the edge intrinsic torque plotted against the mid-radius toroidal velocity for two different β_N values. One can clearly see that the intrinsic drive remains active even with large external NBI torque and rapid rotation. Curiously, the intrinsic torque actually appears to be enhanced as the rotation is increased in the co- I_p direction. This is somewhat surprising, since one should at least expect a (small) reduction in the pedestal $E \times B$ shear as the rotation is increased, since for these DIII-D conditions, the $V_\phi B_\theta$ contribution to the radial electric field from force balance opposes the ∇P term.

From the slope of the lines of best fit, there is ≈ 0.1 Nm enhancement in the edge intrinsic torque for every 100 km/s increase in the toroidal velocity at mid-radius.

To more directly measure the edge intrinsic drive, detailed measurements have been made using a reciprocating Mach probe in the edge of both L-mode and low powered H-mode plasmas (during a slowly evolving ELM-free period). When the injected power is kept close to the 1 MW level, the probe is able to penetrate about 1 cm inside the separatrix. As shown in Fig. 3, a highly localized region of rotation is clearly observed at the edge, which develops within 50 ms of the L-H transition, at a time when the core rotation (as measured by charge exchange recombination) is still negligible [16]. Although in this particular dataset, the formation of the edge layer appears to be triggered by the L-H transition, other data obtained in upper single null configuration show the layer can exist even in L-mode plasmas [17].

The probe also measures fluctuation quantities [18], including the turbulent Reynolds stress. Unexpectedly, in these low power discharges, the turbulent Reynolds stress at the boundary is approximately zero. This implies that an additional mechanism separate to residual stress is required in order to understand intrinsic rotation.

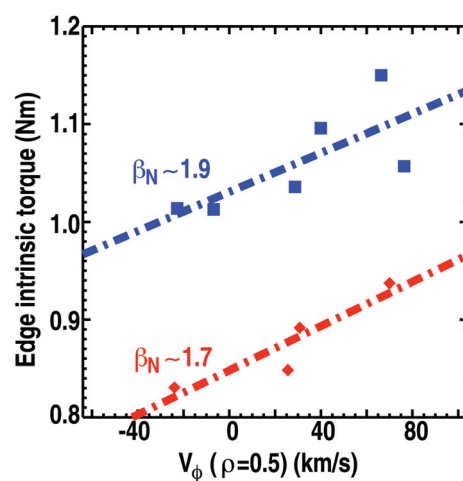


FIG. 2. Edge intrinsic torque ($\rho > 0.8$) as a function of toroidal velocity at mid-radius for two different β_N levels. Here, positive V_ϕ is in the co- I_p direction.

A simple model developed to estimate the net velocity resulting from thermal ion orbit loss of counter-current going ions [10] appears to at least qualitatively describe the magnitude and radial extent of the edge localized peak in toroidal rotation, as shown in Fig. 3. Given the reasonable agreement achieved from this simplified analytic approach, it appears that for these low power H-mode plasmas, thermal orbit losses may play a role in the formation of the intrinsic rotation profile.

However, it is also clear that this mechanism alone cannot explain all tokamak intrinsic rotation data; for one thing, orbit losses always result in co-current rotation, whereas counter intrinsic rotation has been observed depending on the density [19,20]. Furthermore, it does not appear to adequately describe data from more typical (higher power) H-mode plasmas, such as those shown in Fig. 1. A measure of an orbit loss torque is made by estimating the rate at which collisions drive the empty loss cone distribution toward becoming a Maxwellian, $\eta \sim v m n \langle R^2 \rangle \omega$, where v is the collisional slowing frequency. This torque can be relatively large, because of the large deviation from being a Maxwellian, and is clearly sensitive to the choice of v . The comparison between this calculation and the measured intrinsic torque is shown in Fig. 4. The model shows weak if any correlation with the experimentally determined intrinsic torque (linear correlation coefficient < 0.5). In fact, the model predicts an intrinsic torque that is nearly independent of the pressure gradient. To some extent, the regression analysis of the intrinsic torque presented in Ref. 15,

$$T_{\text{intrinsic}}^{\text{edge}} = 0.255 - 2.79 \times 10^{-3} \nabla P \quad (2)$$

already suggested that separate mechanisms may be responsible for setting up the edge intrinsic rotation, as indicated by the need for an offset term in addition to the linear dependence on the pressure gradient. We may speculate that perhaps the offset term is a result of thermal ion orbit losses, which is supported by the fact that the calculated torque based on such a model is almost independent of the H-mode pedestal properties, while the ∇P dependence is associated with residual stress arising from $E \times B$ shear. Further reinforcing this idea, modeling has been performed on a companion set of three L-mode discharges: ECH only, co-NBI and counter-NBI [17]. The analysis finds that the edge intrinsic torque closely matches the predicted value based on the expression Eq. (2) using the (L-mode) plasma pressure gradients. However, the intrinsic torque in these L-mode plasmas ($T_{\text{intrinsic}}^{\text{edge}} \sim 0.3$ Nm) comes almost entirely from the offset in the regression analysis. This apparent change in the relative roles of thermal ion orbit loss and $E \times B$ -driven residual stress as one moves from low power plasmas to higher β_N

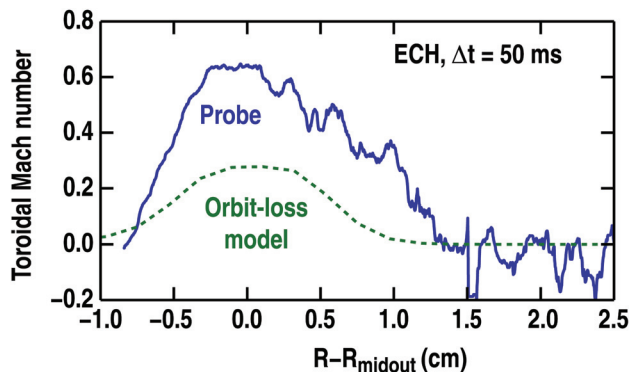


FIG. 3. Probe measurement of toroidal Mach number profile near the boundary, compared with the prediction from a simple orbit loss model.

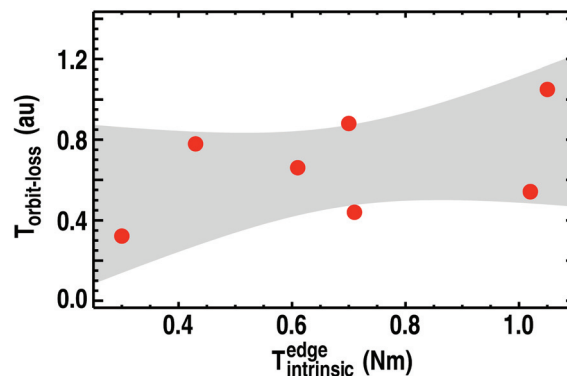


FIG. 4. Comparison of measured intrinsic torque from Fig. 1 with torque predicted from simple orbit loss model.

clearly needs to be properly resolved before a quantitative understanding of intrinsic rotation can be claimed and used for extrapolation to ITER.

3. Intrinsic Torque Inside of Mid-Radius

In principle, residual stress transport may be active in the core of the plasma as well, and can therefore lead to modifications of the core intrinsic rotation profile. Generally, $E \times B$ shear is likely to be smaller in the core than at the edge, although plasmas with strong internal transport barriers may still allow this to play a role. As such, we may expect other documented effects, such as up-down asymmetries [8] or charge separation [9], to play a relatively more important role in intrinsic rotation drive in the core.

Figure 1 shows the integrated torque density from the plasma center out to mid-radius, i.e. $T_{\text{intrinsic}}^{\text{core}} = \int_{\rho=0}^{0.5} \eta_{\text{intrinsic}} dV$, for the shots presented in Fig. 1. It is clear that the magnitude of intrinsic drive for typical H-mode plasmas is very weak compared with the edge, in most cases barely outside of the error bars. The core intrinsic torque is sufficiently small that no clear correlation with the local ∇P can be discerned.

Even though the core intrinsic torque tends to be small compared with the edge, some cases have been found where it is large enough to modify the rotation profile. For example, large intrinsic torques have been observed in the core of QH-mode plasmas, a mode of operation characterized by an H-mode edge, but with increased edge transport provided by a quasi-coherent saturated MHD mode near the edge dubbed the edge harmonic oscillation [21]. Since QH-mode plasmas typically operate with rapid toroidal rotation, the technique outlined in Sec. 2 has been exploited to infer the intrinsic torque profile. The ability to measure the intrinsic torque in these QH-mode plasmas has been instrumental in understanding why QH-modes with low counter neutral beam torque maintain a counter rotation, despite having edge pedestals that would suggest that a co-intrinsic torque should dominate the angular momentum balance. Figure 5 shows the intrinsic torque density and integrated intrinsic torque, $T_{\text{intrinsic}}(\rho) = \int_0^\rho \eta_{\text{intrinsic}} dV$, and indeed a co-intrinsic torque is observed at the edge, $T_{\text{intrinsic}}^{\text{edge}} = T_{\text{intrinsic}}(1) - T_{\text{intrinsic}}(0.8) \sim 0.8$ Nm. More importantly, there is a significant counter intrinsic torque across most of the core profile, which helps explain the large counter rotation in QH-mode. The net result is a total intrinsic torque which is relatively small, and is actually in the counter I_p direction.

Figure 6 shows another example of a plasma with counter intrinsic torque in the core, this time from a hybrid scenario discharge with dominant co-NBI. Again, the standard co-intrinsic torque at the edge common to all H-modes is seen, closely matching the expected torque from Eq. (2). But similar to the QH-mode plasma, a counter intrinsic torque is also observed across an extended region of the plasma. One must be a little cautious of the interpretation of the counter intrinsic torque in this case. It is well-documented that hybrid discharges are typically associated with core neoclassical tearing modes (NTMs), which are tightly coupled with the rotation. Indeed, such modes must exert a drag on the rotation (so for a co-rotating plasma, this appears as a counter

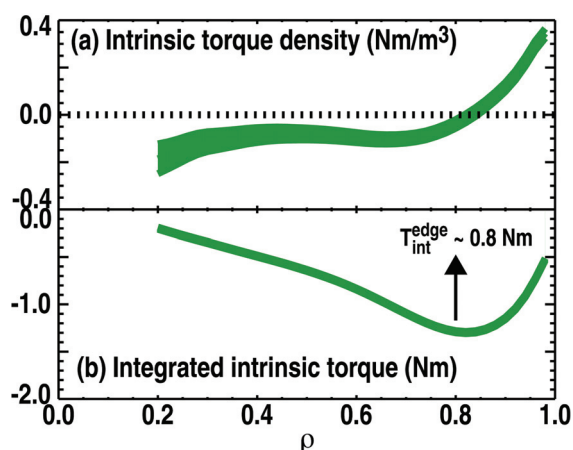


FIG. 5. (a) QH-mode intrinsic torque profile showing typical H-mode edge intrinsic drive, but with an extended radial region of counter intrinsic torque throughout the core. (b) Integrated intrinsic torque, showing net counter intrinsic torque to the edge.

torque), and moreover, the mode amplitude increase as the rotation slows [22], setting up a possible positive feedback loop. So it is conceivable that the “missing” torque extracted using the NBI torque-step technique is nothing more than the unaccounted for drag from the NTM. However, it is important to point out that other hybrid plasmas with larger NTM amplitudes have been similarly analyzed and find no significant core counter torque.

The intrinsic torque profile in Fig. 7 exhibits some interesting properties that are worth expounding. In particular, for a plasma with no external momentum input such as conceivably a future DEMO reactor, the generation of such a intrinsic torque would inherently produce a sheared rotation profile. However, quite differently than present-day experiments, the resultant rotation profile would be very different, with the core plasma rotating in the counter current direction, while the pedestal would rotate in co-direction, with a strong shear layer necessarily connecting the two regions.

Figure 7 shows data suggesting that ECH is capable of modifying the intrinsic drive in the core in some circumstances. Empirical evidence that ECH can generate counter intrinsic torques in the core has existed for some time; for example, hollow intrinsic rotation profiles as reported in Ref. 23. However, the data presented in Fig. 7 represents a more direct measurement of core intrinsic torque modifications due to ECH. The measurements were made in typical lower single null H-mode plasmas, with $I_p \sim 1.25$ MA, $B_T \sim 1.9$ T and $\beta_N \sim 1.8$. A three point ECH deposition scan was performed, with approximately 2.2 MW of power deposited predominantly at $\rho_{ECH} \sim 0.2$ and 0.5 for two conditions. For the third case, ECH power was deposited simultaneous at these two locations, with comparable power deposited in each lobe as calculated by TORAY (achieved by increasing the ECH power to about 3.5 MW). As can be seen in Fig. 8, when moderate power is deposited in either location, the core intrinsic torque is inferred to be essentially zero within error bars, as typically observed in H-mode. However, when power is spread out between the two locations, a significant counter torque in the core is observed. It is not clear from this data whether the counter torque is a result of the spread torque deposition, or the increased power, although there are reasonable indications from other shots that it is the power level that is critical. Interestingly, ECH has also been reported to modify the intrinsic rotation on JT-60U [24], however, the effect was exactly the opposite than reported here, namely with the ECH driving co-intrinsic rotation.

The thus-far limited set of plasmas exhibiting significant levels of intrinsic drive in the core has made it difficult to identify a common link that may be responsible for this effect. However, it appears that no single parameter can account for the generation of core intrinsic

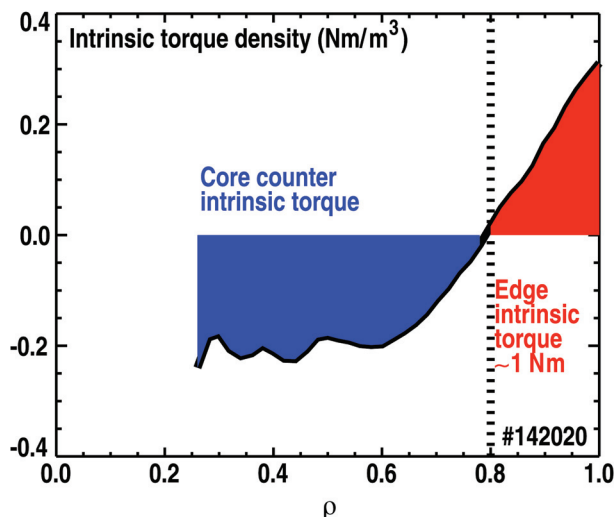


FIG. 6. Intrinsic torque density profile of a hybrid scenario discharge, showing significant counter drive in the core.

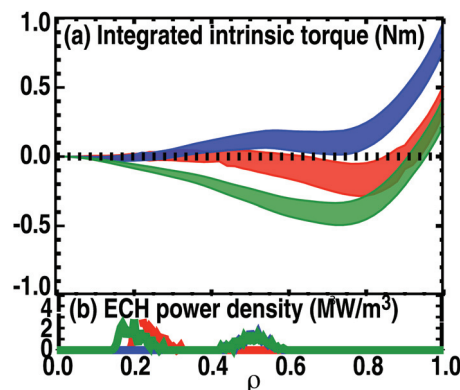


FIG. 7. (a) Intrinsic torque for H-mode plasmas with different ECH locations, with deposition profile as calculated by TORAY in (b).

torque. In particular, core intrinsic torque has been observed in both upper and lower single null shapes, and consideration of q_{\min} , q_{95} , magnetic shear, I_p and β_N and local $E \times B$ shearing rate does not serve to predict whether a plasma will have core intrinsic drive. Many plasmas with core intrinsic torque exhibit some form of coherent MHD (e.g. NTMs in hybrids, EHO in QH-mode plasmas), and typically a notable neutron deficiency comparing the measured and TRANSP calculated rate. Still, a plasma with such properties does not automatically display intrinsic drive in the core, and simple H-mode plasmas such as the ECH case in Fig. 7 with no such MHD can still have core intrinsic torque.

It is clear that the physics of the intrinsic torque in the core of the plasma is an extremely complicated phenomenon, and it is not obvious that an empirical experimental approach will be sufficient to unravel the contributing factors. As such, gyrokinetic simulations with GYRO [25] have been undertaken to try to understand intrinsic drive in the core. However, it is somewhat problematic to meaningfully simulate the residual stress driven torque. The pedestal is generally outside the usual radial region used in the code (primarily because the inherent ordering that the gyroradius is small compared with the gradient scale lengths breaks down), while in the core, cases with significant core torque are often not well-suited to simulation (e.g. ion-temperature gradient turbulence stabilized in hybrid plasmas). A further complication arises due to the well-documented sensitivity of the simulated flows to small variations in the gradient scale lengths. As such, the simulation is limited to comparing the computed ratio of the toroidal angular momentum flow to the power flow, M/P , to the experimental quantity. An example GYRO analysis of residual stress is illustrated in Fig. 8. In this DIII-D shot, the toroidal rotation is essentially zero within experimental error (both V_ϕ and dV_ϕ/dr). GYRO simulations show that the small remaining toroidal rotation makes only a negligible contribution to the experimental level M/P which by definition is nearly all residual stress. There are three contributions to residual stress considered here (assuming perfect toroidal symmetry): shear in the $E \times B$ velocity [4,5]; up-down asymmetry [6]; and profile variation (mostly) in the density and temperature gradients which we call *profile shear*. (The last of these is implicitly turned off in “flat profile” GYRO simulations). Turning off all these residual stress components, the small M/P drive from the small toroidal rotation is shown in the blue curve of Fig. 8. The residual stress drive from up-down asymmetry alone (green) is very small. The small diamagnetic level $E \times B$ shear (which can be independently turned off) makes only a small contribution. In this particular case, profile shear appears to be the largest contribution. The apparent good agreement with experiment (red) when all momentum transport mechanisms are operative (brown) is somewhat fortuitous. Small 10% level uncertainty in the density and temperature gradients can dramatically change the simulated M/P profile (even including flipping the sign across the profile). To fully validate low rotation (residual stress) gyrokinetic momentum transport theory, global transport balance simulations are required in which the temperature and density profiles are “tweaked” so the simulated and experimental energy and particle flows are in balance [26]. These are in progress.

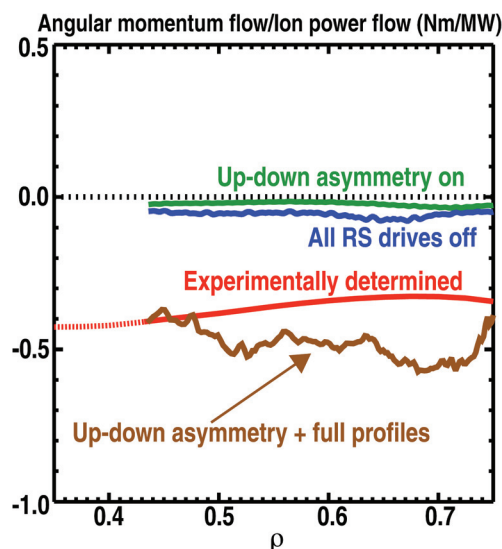


FIG. 8. Comparison of experimental momentum flow as determined by TRANSP (red) with GYRO simulations: full geometry and profiles (brown); full geometry, but flat profiles (green); all residual stress drives turned off (blue).

4. Conclusions

A clearer understanding of the generation of intrinsic rotation in fusion plasmas is developing. In the edge, a clear correlation is observed between the intrinsic torque and the pedestal pressure gradient, which is suggestive that residual stress, resulting, for example, through $E \times B$ shear, may be a key player. However, probe measurements indicate that, at least in low power H-modes, the turbulent Reynolds stress alone may be inadequate to describe the formation of the intrinsic rotation layer at the edge. A simple model considering thermal ion orbit loss at the edge appears to qualitatively describe the probe velocity measurements in these conditions, but does not readily explain the broader ∇P dependence of the edge intrinsic torque in H-mode. Therefore, it is apparent that multiple mechanisms likely contribute to the overall intrinsic rotation at the edge.

The picture is even more complicated in the core. Although the core intrinsic torque is typically found to be small, a few conditions exist where significant intrinsic drive is manifested. These include certain advanced operating regimes, such as hybrid and QH-mode plasmas, and the application of ECH also appears capable of modifying the intrinsic torque in the core. At present, the mechanisms for generating intrinsic torque in the core have not been quantitatively identified, but the existence of core intrinsic torque cannot be simply predicted based on simple scalar quantities characterizing the plasma.

This work was supported by the US Department of Energy under DE-AC02-76CH03073, DE-FC02-04ER54698, DE-FG02-89ER53296, SC-G903402, and DE-FG02-89ER53297.

References

- [1] STRAIT, E.J., *et al.*, Phys. Rev. Lett. **74** (1995) 2483
- [2] BURRELL, K.H., Phys. Plasmas **4** (1997) 1499
- [3] RICE, J.E., *et al.*, Nucl. Fusion **38** (1998) 75
- [4] DOMINGUEZ, R.R and STAEBLER, G.M., Phys. Fluids B **5** (1993) 3876
- [5] GÜRCAN, Ö.D., *et al.*, Phys. Plasmas **14** (2007) 042306
- [6] CAMENEN, Y., *et al.*, Phys. Rev. Lett. **102** (2009) 125001
- [7] DIAMOND, P.H., *et al.*, Phys. Plasmas **15** (2008) 012303
- [8] McDEVITT, C.J., *et al.*, Phys. Rev. Lett. **103** (2009) 205003
- [9] WANG, W.X., *et al.*, Phys. Plasmas **17** (2010) 072511
- [10] deGRASSIE, J.S. *et al.*, Nucl. Fusion **49** (2009) 085020
- [11] SOLOMON, W.M., *et al.*, Plasma Phys. Control. Fusion **49** (2007) B313
- [12] HAWRYLUK, R., *Phys. Plasmas Close to Thermonuclear Conditions*, B. Coppi, *et al.*, Editor (CEC, Brussels, 1980) Vol. 1, pp. 19–46
- [13] GOLDSTON, R.J., *et al.*, J. Comput. Phys. **78** (1981) 61
- [14] PANKIN, A., Comput. Phys. Commun. **159** (2004) 157
- [15] SOLOMON, W.M., *et al.*, Phys. Plasmas **17** (2010) 056108
- [16] MULLER, S.H., *et al.*, to be submitted to Phys. Rev. Lett. (2010)
- [17] BOEDO, J.A., *et al.*, submitted to Phys. Plasmas (2010)
- [18] WATKINS, J.G., *et al.*, Rev. Sci. Instrum. **63** (1992) 4728.
- [19] BORTOLON, A., *et al.*, Phys. Rev. Lett. **97** (2006) 235003
- [20] RICE, J.E., *et al.*, Plasma Phys. Control. Fusion **50** (2008) 124042
- [21] BURRELL, K.H., *et al.*, Phys. Plasmas **8** (2001) 2153
- [22] POLITZER, P.A., *et al.*, Nucl. Fusion **48** (2008) 075001
- [23] deGRASSIE, J.S., *et al.*, Phys. Plasmas **14** (2007) 056115
- [24] YOSHIDA, M., *et al.*, Phys. Rev. Lett. **103** (2009) 065003
- [25] CANDY, J. and WALTZ, R.E., J. Comput. Phys. **186** (2003) 545
- [26] WALTZ, R.E., *et al.*, Nucl. Fusion **45** (2005) 741